

# Large-Scale Fabrication of Pr<sup>3+</sup> Doped or Undoped Nanosized ATiO<sub>3</sub> (A = Ca, Sr, Ba) with Different Shapes via a Facile Solvothermal Technique

Xianmin Zhang,<sup>†,‡</sup> Jiahua Zhang,<sup>\*,†</sup> Ye Jin,<sup>†,‡</sup> Haifeng Zhao,<sup>†</sup> and Xiao-jun Wang<sup>\*,†,§</sup>

Key Laboratory of Excited State Processes, Changchun Institute of Optics, Fine Mechanics and Physics, Chinese Academy of Sciences, 16 Eastern South Lake Road, Changchun 130033, China, Graduate School of Chinese Academy of Sciences, Beijing, 100039, China, Department of Physics, and Georgia Southern University, Statesboro, Georgia 30460

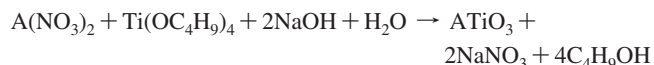
Received October 16, 2007; Revised Manuscript Received January 6, 2008

**ABSTRACT:** CaTiO<sub>3</sub> nanoflowers, SrTiO<sub>3</sub> nanocubes, and BaTiO<sub>3</sub> nanospheres have been prepared by an environmentally friendly solvothermal technique and structurally characterized by X-ray diffraction and field emission scanning electron microscopy. Red fluorescence originating from intra 4f <sup>1</sup>D<sub>2</sub>-<sup>3</sup>H<sub>4</sub> transition of Pr<sup>3+</sup> is observed by doping Pr<sup>3+</sup> ions in CaTiO<sub>3</sub> nanoflowers. The energy transfer and red emission processes of Pr<sup>3+</sup> in CaTiO<sub>3</sub>:Pr<sup>3+</sup> nanoflowers are discussed.

## Introduction

Low-dimensional nanostructures have attracted extensive interest due to their novel size- and shape-dependent properties and potential applications in numerous areas such as nanoscale electronics and photonics.<sup>1–4</sup> Much effort has been directed toward synthesizing carbon nanotubes,<sup>1</sup> semiconductors,<sup>2</sup> metallic,<sup>3</sup> and binary oxide nanowires,<sup>4</sup> and nanobelts.<sup>5</sup> In recent years, nanoscale ternary transition metal oxides, ATiO<sub>3</sub> (A = Ca, Sr, Ba), with a perovskite structure, have received great attention because of their interesting properties and promising application in microwave-tunable devices<sup>6</sup> and transducers as well as logic circuitry,<sup>7</sup> etc. Thus, considerable efforts have been devoted to fabricate nanosized SrTiO<sub>3</sub> and BaTiO<sub>3</sub> with different shapes such as nanoparticles,<sup>8</sup> nanocubes,<sup>9</sup> nanowires,<sup>9</sup> nanorods,<sup>10</sup> etc. Comparatively little work has been performed on the fabrication of shape-dependent CaTiO<sub>3</sub>. However, the previous synthesis methods are complicated because of numerous reagents. Moreover, the relatively high reaction temperature increases the cost of the synthesis. Here, we develop an environmentally friendly solvothermal technique to prepare first homogeneous CaTiO<sub>3</sub> nanoflowers. On the basis of this method, SrTiO<sub>3</sub> nanocubes and BaTiO<sub>3</sub> nanospheres have also been successfully prepared.

The synthesis of ATiO<sub>3</sub> was carried out according to the overall formal reaction:



In our experimental procedure, 0.02 M alkali metals nitrate (Ca(NO<sub>3</sub>)<sub>2</sub>·4H<sub>2</sub>O, Sr(NO<sub>3</sub>)<sub>2</sub> or Ba(NO<sub>3</sub>)<sub>2</sub>) and 0.3 M NaOH were dissolved in the ethanol and distilled water solution with molar ratio of 1:9. (The production has the highest yield at this ratio.) Under constant magnetic stirring, Ti(OC<sub>4</sub>H<sub>9</sub>)<sub>4</sub> 0.02 M was added dropwise. To reduce the hydrolytic rate of Ti(OC<sub>4</sub>H<sub>9</sub>)<sub>4</sub>, the solution was kept cold by an ice–water mixture. After the solution was stirred for 15 min, a milky colloid solution was transferred into closed Teflon-lined autoclaves of 50 mL capacity, which were filled ca. 85% of the total volume. The tank was maintained at 180 °C for 10 h (CaTiO<sub>3</sub> and BaTiO<sub>3</sub>) and 200 °C for 4 h (SrTiO<sub>3</sub>), respectively, and then cooled to room temperature. The heating rate

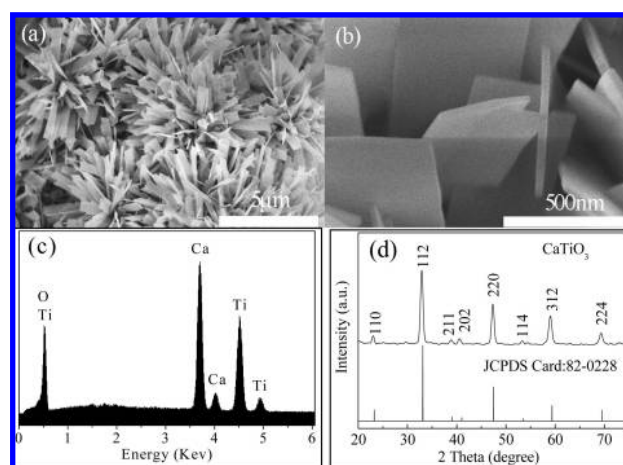


**Figure 1.** FESEM images of CaTiO<sub>3</sub> nanoflowers: (a) Low-magnification; (b) high-magnification. (c) EDS spectra of CaTiO<sub>3</sub> nanoflowers. (d) XRD spectra of CaTiO<sub>3</sub> nanoflowers.

was 5 °C/min. The products were collected by centrifuge, washed several times using distilled water, and dried at 65 °C under vacuum. The products are amorphous if the solvothermal temperature is below 180 °C.

The morphology of the synthesized products was characterized by field emission scanning electron microscopy (FESEM, Hitachi S-4800). The structural characterization was analyzed by X-ray diffraction (XRD; Rigaku D/max-rA) spectroscopy with the Cu Kα line of 1.540 78 Å. Energy dispersive spectroscopy (EDS) was performed on a GENESIS2000XMS 60S (EDAX Inc.). Photoluminescence (PL) and PL excitation (PLE) spectra were measured using Hitachi F-4500 fluorescence spectrophotometer.

Figure 1a shows the FESEM images of CaTiO<sub>3</sub> nanoflowers. It is evident that the CaTiO<sub>3</sub> product mainly consists of homogeneous, straight, smooth and striplike structures. From the FESEM results (Figure 1b), every strip of the nanoflowers is 3–4 μm in length and 300–400 nm in width, and their thickness is quite thin, about 30 nm. To determine the composition of the nanoflowers, an EDS spectrum is presented in Figure 1c. It is found that the nanoscripts are composed of Ca, Ti, and O. The XRD pattern (Figure 1d) indicates the formation of orthorhombic CaTiO<sub>3</sub> (JCPDS Card No. 82-0228).

\* To whom correspondence should be addressed. E-mail: zhangjh@ciomp.ac.cn or xwang@georgiasouthern.edu.

<sup>†</sup> Changchun Institute of Optics, Fine Mechanics and Physics, Chinese Academy of Sciences.

<sup>‡</sup> Graduate School of Chinese Academy of Sciences.

<sup>§</sup> Georgia Southern University.

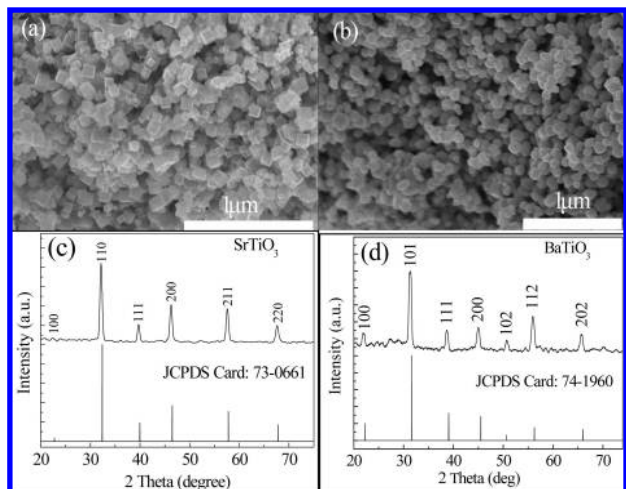


**Figure 2.** FESEM images of (a) SrTiO<sub>3</sub> nanocubes and (b) BaTiO<sub>3</sub> nanospheres. XRD spectra of (c) SrTiO<sub>3</sub> nanocubes and (d) BaTiO<sub>3</sub> nanospheres.

With the same methods, SrTiO<sub>3</sub> nanocubes and BaTiO<sub>3</sub> nanospheres have also been successfully prepared. The uniform SrTiO<sub>3</sub> nanocubes (Figure 2a) and BaTiO<sub>3</sub> nanospheres (Figure 2b) are observed with an average size of 90 and 85 nm. The XRD patterns indicate the formation of cubic SrTiO<sub>3</sub> (JCPDS Card No. 73-0661) and tetragonal BaTiO<sub>3</sub> (JCPDS Card No. 74-1960), as shown in Figure 2, panels c and d, respectively. The EDS spectra of the SrTiO<sub>3</sub> (Figure S1a) and BaTiO<sub>3</sub> (Figure S1b) indicate that these nanocubes and nanospheres are composed of Sr, Ti and O or Ba, Ti and O.

Low-dimensional nanomaterials doped with rare earth ions have received considerable interest due to their potential applications not only in luminescent and displays devices<sup>11</sup> but also as a probe to investigate the microstructure of nanocrystals.<sup>12</sup> In previous work, bulk perovskite-type oxides doped with rare earth ions have been extensively studied,<sup>13</sup> However, few reports have been presented on preparing rare earth doped ATiO<sub>3</sub> (A = Ca, Sr, Ba) nanophosphors. Recently, our research group has synthesized CaTiO<sub>3</sub>:Pr<sup>3+</sup> nanocubes by an improved sol-gel technique.<sup>14</sup> In the present work, we find that Pr<sup>3+</sup> ions (0.4% PrCl<sub>3</sub> solution was added; the concentration of PrCl<sub>3</sub> is 2.82 mg/mL) can be doped into CaTiO<sub>3</sub> nanoflowers, inducing red emission at 610 nm originating from intra 4f <sup>1</sup>D<sub>2</sub>-<sup>3</sup>H<sub>4</sub> transition of Pr<sup>3+</sup>.

PL ( $\lambda_{\text{ex}} = 323\text{nm}$ ) and PLE ( $\lambda_{\text{em}} = 610\text{nm}$ ) spectra of Pr<sup>3+</sup> doped CaTiO<sub>3</sub> nanoflowers are presented in Figure 3A. As shown in Figure S2, the FESEM observations indicate that the characteristic, expected morphology of the Pr<sup>3+</sup> doped CaTiO<sub>3</sub> samples did not change upon doping. The room temperature PL spectra show a red emission line at 610 nm originating from intra 4f <sup>1</sup>D<sub>2</sub>-<sup>3</sup>H<sub>4</sub> transition of Pr<sup>3+</sup>,<sup>15</sup> demonstrating Pr<sup>3+</sup> ions can be doped into the CaTiO<sub>3</sub> nanoflowers. The PLE spectra monitoring the red emission mainly consists of three broad bands (a, b, and c) in the ultraviolet region, which are located at 323 nm (a), 265 nm (b), and 375 nm (c), respectively. The position of band a is assigned to the band edge absorption of CaTiO<sub>3</sub> host.<sup>15</sup> Bands b and c are attributed to the absorption of Pr<sup>3+</sup> 4f5d states<sup>15b</sup> and a low-lying Pr-to-metal (Pr<sup>3+</sup>-Ti<sup>4+</sup>) intervalence charge transfer state,<sup>16</sup> respectively. Under the 265 nm excitation, there is no 4f5d → 4f<sup>2</sup> luminescence of Pr<sup>3+</sup> in CaTiO<sub>3</sub>:Pr<sup>3+</sup> nanoflowers. It is obvious that a nonradiative relaxation from the lowest 4f5d level to the <sup>1</sup>D<sub>2</sub> state occurs. When an excitation occurs at 323 nm, the spectroscopic behavior of the CaTiO<sub>3</sub>:Pr<sup>3+</sup> nanoflowers can be compared to the behavior of large gap semiconductors such as rare-earth doped ZnS phosphors,<sup>17</sup> since the excitation of the red luminescence is achieved through the conduction band (CB). States of host matrix then transferred to the emitting level of the activator ions. In the case of the CaTiO<sub>3</sub>:Pr<sup>3+</sup> nanoflowers, the UV (323 nm) excitation can generate O(2p)

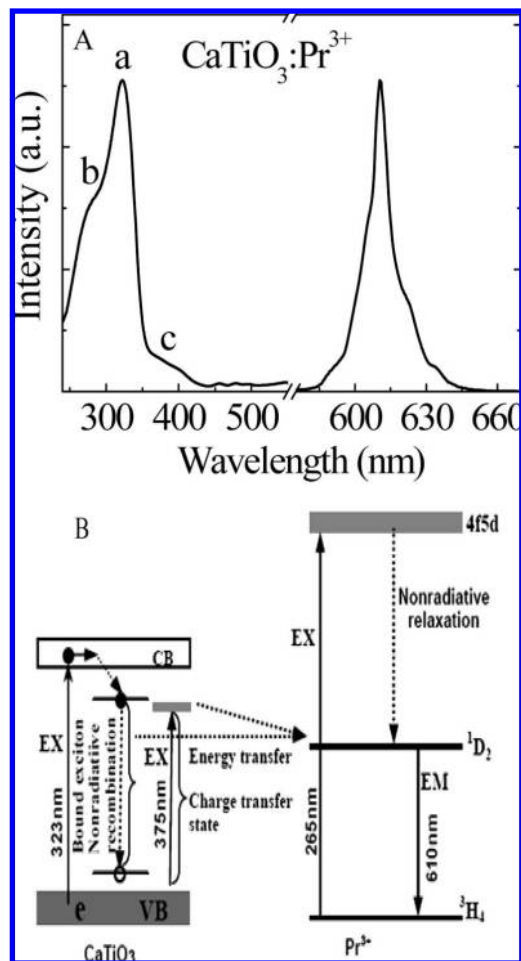


**Figure 3.** (A) PL (right,  $\lambda_{\text{ex}} = 323\text{nm}$ ) and PLE (left,  $\lambda_{\text{em}} = 610\text{nm}$ ) spectra of CaTiO<sub>3</sub>:Pr<sup>3+</sup> nanoflowers. (B) One simple model illustrating the energy transfer to Pr<sup>3+</sup> and the red emission process of Pr<sup>3+</sup>.

→ Ti(3d) and/or Pr<sup>3+</sup> (4f) → Ti(3d) charge transfers and then produces electron-hole pairs, leading to the formation of bound excitons. As no luminescence from the bound exciton recombination is observed, these excitons, if formed, decay nonradiatively through a resonant or quasisonant transfer to the 4f shell of Pr<sup>3+</sup> ions.<sup>15</sup> The excitation band at 375 nm is ascribed to a low-lying Pr<sup>3+</sup>/Ti<sup>4+</sup> ↔ Pr<sup>4+</sup>/Ti<sup>3+</sup> charge transfer state, as the final nonradiative relaxation pathway is to the emitting <sup>1</sup>D<sub>2</sub> level in Pr<sup>3+</sup>-doped CaTiO<sub>3</sub>.<sup>16</sup> One simple model illustrating the energy transfer to Pr<sup>3+</sup> and the red emission process of Pr<sup>3+</sup> is shown in Figure 3B. Although Pr<sup>3+</sup> ions are also experimentally doped in SrTiO<sub>3</sub> nanocubes and BaTiO<sub>3</sub> nanospheres, the red emission cannot be detected. The fluorescence efficiency is very weak in Pr<sup>3+</sup> doped bulk SrTiO<sub>3</sub> and BaTiO<sub>3</sub>,<sup>12c</sup> which is expected to be further reduced due to the presence of numerous nonradiation quenching centers on the surface of nanophosphors.<sup>11</sup> In CaTiO<sub>3</sub>:Pr<sup>3+</sup> nanoflowers, no phosphorescence is observed. This indicates no energy storage traps in nanoflowers.

The present study shows that CaTiO<sub>3</sub> nanoflowers, SrTiO<sub>3</sub> nanocubes, and BaTiO<sub>3</sub> nanospheres can be prepared by an environmentally friendly solvothermal technique. Red fluorescence originating from intra 4f <sup>1</sup>D<sub>2</sub>-<sup>3</sup>H<sub>4</sub> transition of Pr<sup>3+</sup> is observed by doping Pr<sup>3+</sup> ions in CaTiO<sub>3</sub> nanoflowers. The synthetic strategy presented here may be extended to other perovskite nanostructures with different compositions.

**Acknowledgment.** This work is financially supported by the MOST of China (2006CB601104, 2006AA03A138) and the National Natural Science Foundation of China (10574128).

**Supporting Information Available:** EDS spectra of SrTiO<sub>3</sub> nanocubes (Figure S1a) and BaTiO<sub>3</sub> nanospheres (Figure S1b); FESEM image of CaTiO<sub>3</sub>/Pr<sup>3+</sup> (Figure S2). This information is available free of charge via the Internet at <http://pubs.acs.org>.

## References

- (1) (a) Alivisatos, A. P. *Science* **1996**, *271*, 933. (b) Pan, Z. W.; Dai, Z. R.; Wang, Z. L. *Science* **2001**, *291*, 1947. (c) Liang, W.; Bockrath, M.; Bozovic, D.; Hafner, J. H.; Tinkham, M.; Park, H. *Nature* **2001**, *411*, 665. (d) Bockrath, M.; Liang, W.; Bozovic, D.; Hafner, J. H.; Lieber, C. M.; Tinkham, M.; Park, H. *Science* **2001**, *291*, 283.
- (2) (a) Morales, A. M.; Lieber, C. M. *Science* **1998**, *279*, 208. (b) Peng, X.; Manna, L.; Yang, W.; Wickham, J.; Sher, E.; Kadavanich, A.; Alivisatos, A. P. *Nature* **2000**, *404*, 59.
- (3) (a) Park, S.-J.; Kim, S.; Lee, S.; Khim, Z. G.; Char, K.; Hyeon, T. *J. Am. Chem. Soc.* **2000**, *122*, 8581. (b) Puntès, V. F.; Krishnan, K. M.; Alivisatos, A. P. *Science* **2001**, *291*, 2115.
- (4) (a) Huang, M. H.; Wu, Y.; Feick, H.; Tran, N.; Weber, E.; Yang, P. *Adv. Mater.* **2001**, *13*, 113. (b) Lei, Y.; Zhang, L. D.; Fan, J. C. *Chem. Phys. Lett.* **2001**, *338*, 231.
- (5) (a) Ma, C.; Moore, D.; Li, J.; Wang, Z. L. *Adv. Mater.* **2003**, *15*, 228. (b) Sigman, M. B.; Korgel, B. A. *J. Am. Chem. Soc.* **2005**, *127*, 10089.
- (6) (a) Lemanov, V. V.; Sotnikov, A. V.; Smirnova, E. P.; Weinacht, M.; Kunze, R. *Solid State Commun.* **1999**, *110*, 611. (b) Kucheiko, S.; Choi, J. W.; Kim, H. J.; Jung, H. J. *J. Am. Ceram. Soc.* **1996**, *79*, 2739. (c) Hao, J.; Si, W.; Xi, X. X.; Guo, R.; Bhalla, A. S.; Cross, L. E. *Appl. Phys. Lett.* **2000**, *76*, 3100. (d) Cockayne, E.; Burton, B. P. *Phys. Rev. B.* **2000**, *62*, 3735.
- (7) (a) Scott, J. F. *Ferroelectr. Rev.* **1998**, *1*, 1. (b) Hill, N. A. *J. Phys. Chem. B* **2000**, *104*, 6694. (c) Tao, S.; Irvine, J. T. S. *Nat. Mater.* **2003**, *2*, 320. (d) Wessels, B. W. *Annu. Rev. Mater. Sci.* **1995**, *25*, 525.
- (8) (a) Wang, X.; Zhuang, J.; Peng, Q.; Li, Y. D. *Nature* **2005**, *437*, 121. (b) Mao, Y.; Banerjee, S.; Wong, S. S. *Chem. Commun.* **2003**, 408. (c) Hernandez, B. A.; Chang, K.-S.; Fisher, E. R.; Dorhout, P. K. *Chem. Mater.* **2002**, *14*, 480.
- (9) Mao, Y.; Banerjee, S.; Wong, S. S. *J. Am. Chem. Soc.* **2003**, *125*, 15718.
- (10) (a) O'Brien, S.; Brus, L.; Murray, C. B. *J. Am. Chem. Soc.* **2001**, *123*, 12085. (b) Urban, J. J.; Yun, W. S.; Gu, Q.; Park, H. *J. Am. Chem. Soc.* **2002**, *124*, 1186.
- (11) (a) Tissue, B. M. *Chem. Mater.* **1998**, *10*, 2837. (b) Meltzer, R. S.; Feofilov, S. P.; Tissue, B. *Phys. Rev. B.* **1999**, *60*, 14012. (c) Williams, D. K.; Bihari, B.; Tissue, B. M.; Mchale, J. M. *J. Phys. Chem. B* **1998**, *102*, 916.
- (12) (a) Lehmann, O.; Kompe, K.; Haase, M. *J. Am. Chem. Soc.* **2004**, *126*, 14935. (b) Dunbar, T. D.; Warren, W. L.; Tuttle, B. A.; Randall, C. A.; Tsur, Y. *J. Phys. Chem. B.* **2004**, *108*, 908. (c) Kyomen, T.; Sakamoto, R.; Sakamoto, N.; Kunugi, S.; Itoh, M. *Chem. Mater.* **2005**, *17*, 3200.
- (13) (a) Vecht, A.; Smith, D. W.; Chadha, S. S.; Gibbons, C. S. *J. Vac. Sci. Technol.* **1994**, *B12*, 781. (b) Okamoto, S.; Yamamoto, H. *Appl. Phys. Lett.* **2001**, *78*, 655. (c) Zhang, X. M.; Zhang, J. H.; Zhang, X.; Chen, L.; Lu, S. Z.; Wang, X. J. *J. Lumin.* **2007**, *122–123*, 958. (d) Zhang, X. M.; Zhang, J. H.; Zhang, X.; Chen, L.; Luo, Y. S.; Wang, X. J. *Chem. Phys. Lett.* **2007**, *434*, 237.
- (14) Zhang, X. M.; Zhang, J. H.; Nie, Z. G.; Wang, M. Y.; Ren, X. G.; Wang, X. J. *Appl. Phys. Lett.* **2007**, *90*, 151911.
- (15) (a) Diallo, P. T.; Boutinaud, P.; Mahiou, R.; Cousseins, J. C. *Phys. Status Solidi* **1997**, *A160*, 255. (b) Liu, X. M.; Jia, P. Y.; Lin, J.; Li, G. Z. *J. Appl. Phys.* **2006**, *99*, 124902.
- (16) Boutinaud, P.; Pinel, E.; Dubois, M.; Vink, A. P.; Mahiou, R. *J. Lumin.* **2005**, *111*, 69.
- (17) Swiatek, K.; Godlewski, M.; Hommel, D. *Phys. Rev. B.* **1990**, *42*, 3628.

CG701023X